

# Diode-pumped alexandrite ring laser in single-longitudinal mode operation for atmospheric lidar measurements

A. MUNK,<sup>1,\*</sup> B. JUNGBLUTH,<sup>1</sup> M. STROTKAMP,<sup>1</sup> H.-D. HOFFMANN,<sup>1</sup> R. POPRAWA,<sup>1,2</sup> J. HÖFFNER,<sup>3</sup> AND F.-J. LÜBKEN<sup>3</sup>

<sup>1</sup>Fraunhofer Institute for Laser Technology, Steinbachstr. 15, 52074 Aachen, Germany

<sup>2</sup>Chair for Laser Technology LLT - RWTH Aachen University, Steinbachstr. 15, 52074 Aachen, Germany

<sup>3</sup>Leibniz Institute of Atmospheric Physics, Schlossstraße 6, 18225 Kühlungsborn, Germany

\*alexander.munk@ilt.fraunhofer.de

**Abstract:** We present, to the best of our knowledge, design and performance data of the first diode-pumped Alexandrite ring laser in Q-switched single-longitudinal mode (SLM) operation. The laser resonator contains two Alexandrite crystals, which are pumped longitudinally by means of two laser diode-bar modules emitting at 636 nm. Single-longitudinal mode operation is achieved by seeding the laser with a diode laser operating in SLM and actively stabilizing the cavity, yielding a linewidth of  $< 10$  MHz at the potassium resonance line at 770 nm. The pulse energy is 1 mJ at a repetition rate of 150 Hz and 0.65 mJ at 320 Hz. The beam quality of  $M^2 < 1.2$  in both directions remains unchanged for the different repetition rates. After characterization in the laboratory, the laser was implemented in a novel mobile lidar system and first atmospheric measurements were conducted successfully.

© 2018 Optical Society of America under the terms of the [OSA Open Access Publishing Agreement](#)

**OCIS codes:** (140.3480) Lasers, diode-pumped; (140.3560) Lasers, ring; (140.3600) Lasers, tunable; (140.3540) Lasers, Q-switched; (140.3570) Lasers, single-mode; (280.3640) Lidar.

## References and links

1. J. Höffner and C. Fricke-Begemann, "Accurate lidar temperatures with narrowband filters," *Opt. Lett.* **30**(8), 890–892 (2005).
2. J. Lautenbach, J. Höffner, P. Menzel, and P. Keller, "The new scanning iron lidar, current state and future developments," in *Proceedings of the 17th ESA Symposium on European Rocket and Balloon Programmes and Related Research*, B. Warmbein (ESA, 2005), pp. 327–329.
3. V. Wulfmeyer and J. Bösenberg, "Single-mode operation of an injection-seeded alexandrite ring laser for application in water-vapor and temperature differential absorption lidar," *Opt. Lett.* **21**(15), 1150–1152 (1996).
4. U. von Zahn and J. Höffner, "Mesopause temperature profiling by potassium lidar," *Geophys. Res. Lett.* **23**(2), 141–144 (1996).
5. J. Höffner and F.-J. Lübken, "Potassium lidar temperatures and densities in the mesopause region at Spitsbergen (78°N)," *J. Geophys. Res.* **112**(D20), D20114 (2007).
6. F.-J. Lübken, J. Höffner, T. P. Viehl, B. Kaifler, and R. J. Morris, "First measurements of thermal tides in the summer mesopause region at Antarctic latitudes," *Geophys. Res. Lett.* **38**(24), L24806 (2011).
7. J. A. McKay and T. D. Wilkerson, "Diode-pumped alexandrite laser for DIAL and Doppler lidar," *Proc. SPIE* **3127**, 124–132 (1997).
8. M. Damzen, "Diode-pumped Alexandrite laser: a bright prospect for future space Lidar missions," *Proc. SPIE* **8534B**, 81 (2012).
9. R. Scheps, B. M. Gately, J. F. Myers, J. S. Krasinski, and D. F. Heller, "Alexandrite laser pumped by semiconductor lasers," *Appl. Phys. Lett.* **56**(23), 2288–2290 (1990).
10. R. Scheps, J. F. Myers, T. R. Glesne, and H. B. Serreze, "Monochromatic end-pumped operation of an Alexandrite laser," *Opt. Commun.* **97**(5–6), 363–366 (1993).
11. A. Teppitaksak, A. Minassian, G. M. Thomas, and M. J. Damzen, "High efficiency  $> 26$  W diode end-pumped Alexandrite laser," *Opt. Express* **22**(13), 16386–16392 (2014).
12. M. Strotkamp, U. Witte, A. Munk, A. Hartung, S. Gausmann, S. Hengesbach, M. Traub, H.-D. Hoffmann, J. Höffner, and B. Jungbluth, "Broadly tunable, longitudinally diode-pumped Alexandrite laser," *Proc. SPIE* **8959**, 89591G (2014).



13. I. Yorulmaz, E. Beyatli, A. Kurt, A. Sennaroglu, and U. Demirbas, "Efficient and low-threshold Alexandrite laser pumped by a single-mode diode," *Opt. Mater. Express* **4**(4), 776–789 (2014).
14. A. Munk, B. Jungbluth, M. Strotkamp, H.-D. Hoffmann, R. Poprawe, and J. Höffner, "Diode-pumped Alexandrite ring laser for lidar applications," *Proc. SPIE* **9726**, 97260I (2016).
15. G. M. Thomas, A. Minassian, X. Sheng, and M. J. Damzen, "Diode-pumped Alexandrite lasers in Q-switched and cavity-dumped Q-switched operation," *Opt. Express* **24**(24), 27212–27224 (2016).
16. U. Parali, X. Sheng, A. Minassian, G. Tawy, J. Sathian, G. M. Thomas, and M. J. Damzen, "Diode-pumped Alexandrite laser with passive SESAM Q-switching and wavelength tenability," *Opt. Commun.* **410**, 970–976 (2018).
17. S. Ghanbari, K. A. Fedorova, A. B. Krysa, E. U. Rafailov, and A. Major, "Femtosecond Alexandrite laser passively mode-locked by an InP/InGaP quantum-dot saturable absorber," *Opt. Lett.* **43**(2), 232–234 (2018).
18. C. Cihan, A. Muti, I. Baylam, A. Kocabas, U. Demirbas, and A. Sennaroglu, "70 femtosecond Kerr-lens mode-locked multipass-cavity Alexandrite laser," *Opt. Lett.* **43**(6), 1315–1318 (2018).
19. P. Pichon, A. Barbet, J. P. Blanchot, F. Druon, F. Balembois, and P. Georges, "LED-pumped alexandrite laser oscillator and amplifier," *Opt. Lett.* **42**(20), 4191–4194 (2017).
20. V. Evtuhov and A. E. Siegman, "A "Twisted-Mode" Technique for Obtaining Axially Uniform Energy Density in a Laser Cavity," *Appl. Opt.* **4**(1), 142–143 (1965).
21. K. Nicklaus, V. Morasch, M. Hoefer, J. Luttmann, M. Vierkötter, M. Ostermeyer, J. Höffner, C. Lemmerz, and D. Hoffmann, "Frequency stabilization of Q-switched Nd:YAG oscillators for airborne and spaceborne lidar systems," *Proc. SPIE* **6451**, 64511L (2007).

## 1. Introduction

Understanding temperature distributions in the atmosphere at altitudes between 80 and 110 km, called the MLT (Mesosphere and lower Thermosphere), is crucial for performing numerical simulations of the Earth's climate. One well-established approach to provide such data is to measure the Doppler broadened line width of metal atoms, e.g. of the potassium resonance line at 770 nm and of the iron resonance line at 386 nm, by means of resonance lidar systems [1,2]. Today, the pulsed lasers used in such systems are flashlamp-pumped Alexandrite ring lasers operating in Q-switched SLM operation [3,4]. The systems are typically operated under rough environmental conditions such as on research ships or in polar regions [4–6]. Due to these conditions and the remote locations, it is essential to extend maintenance-free operating times and optimize the wall-plug efficiency of such lasers. One hopeful approach to reach these aims is by replacing the flashlamp pumps with diode lasers [7,8]. The proof-of-principle of longitudinally, diode-pumped Alexandrite lasers was demonstrated in 1990 [9,10]. Recently, with the advance of red diode laser technology, new investigations in the field of diode-pumped Alexandrite lasers have been conducted [11–16]. Other investigations on Alexandrite involve the usage of green lasers as pumping sources for generation of ultra-short pulses [17,18] and LED-pumped Alexandrite lasers [19].

In this work we present design and performance of the, to the best of our knowledge, first Q-switched, diode-pumped Alexandrite ring laser in SLM operation. After the output parameters required for lidar applications were successfully demonstrated in the laboratory, first atmospheric measurements were carried out in a novel mobile lidar system.

## 2. Pump module

The pump modules used in the experiments are commercially available diode lasers. Within the module the beams from seven diode bars are collimated and optically combined to provide 100 W of pulse peak power, as shown in Fig. 1 (a), which corresponds to a pulse energy of 20 mJ at a pulse length of 200  $\mu$ s. Changing the repetition rate from 100 Hz to 500 Hz does not change the peak power significantly. The output wavelength is 636 nm, see the inset in Fig. 1 (a). The module provides an output beam with a beam quality of about  $M^2 = 30$  in fast-axis and  $M^2 = 300$  in slow-axis. The corresponding caustic is plotted in Fig. 1 (b). The beam quality and the peak power are unaffected by the repetition rate up to a duty cycle of 5%.



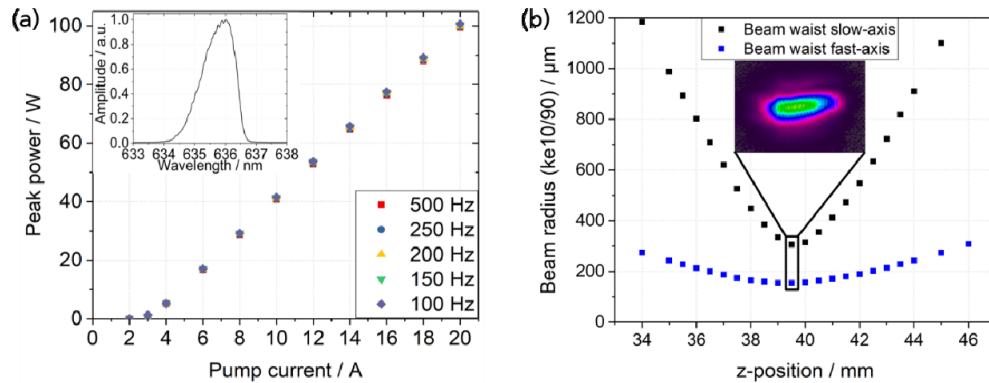


Fig. 1. (a) Pulse peak power as a function of the pump current for different repetition rates and spectrum of the diode pump module at 20 A pump current, 200  $\mu$ s pulse length and a repetition rate of 250 Hz (inlet). (b) Beam caustic in fast-axis and slow-axis behind pump optics and beam profile in the focus (inlet).

A combination of two cylindrical lenses (focal length of + 100 mm) and two spherical lenses (focal length of -100 mm) is used to expand the pump beam in slow-axis and reduce its radius in fast-axis before the beam is focused with a spherical achromatic lens with a focal length of 50 mm. Thereby the output beam of each diode module is shaped to generate pump spots with waist radii of 150  $\mu$ m in fast-axis and 300  $\mu$ m in slow-axis inside the Alexandrite crystals. The total length of the beam shaping from the diode pump module to crystal is 215 mm. The optics design is based on off-the-shelf components and has not yet been optimized for simplicity or compactness.

### 3. Laser design

The envisaged measurement of the potassium resonance line requires a linewidth below 30 MHz and consequently a laser operating in SLM. In this operational mode the spectral properties and the efficiency of lasers with linear resonators suffers from spatial hole burning induced by the standing wave pattern by the counter-propagating waves. The twisted mode technique [20], which can be used in a linear laser resonator to prevent a standing wave pattern, is an issue for Alexandrite due to the birefringent nature of this crystal. To overcome this effect, a travelling wave ring resonator is chosen for single longitudinal mode operation of an Alexandrite laser.

The Alexandrite crystal is longitudinally pumped so that the spatial overlap of the pumped volume of the crystal with the laser mode and, therefore, the laser efficiency is maximized. However, due to the low beam quality and large divergence of the pump beam in the slow-axis, the pump mirror is placed directly in front of the laser medium for the pump light to pass through the aperture without diffraction or even clipping. Since there is such a short distance between the mirror and the crystal's facet, the beam path of the laser mode has to be redirected through the laser medium after its reflection. The incoming and outgoing beams are separated by a small angle and split by means of a scraper mirror to form a ring cavity, as shown in Fig. 2. This geometry also increases the spatial overlap between the laser mode and the highly divergent pump mode in slow-axis and, consequently, the laser gain and prevents lasing in higher transversal mode operation.



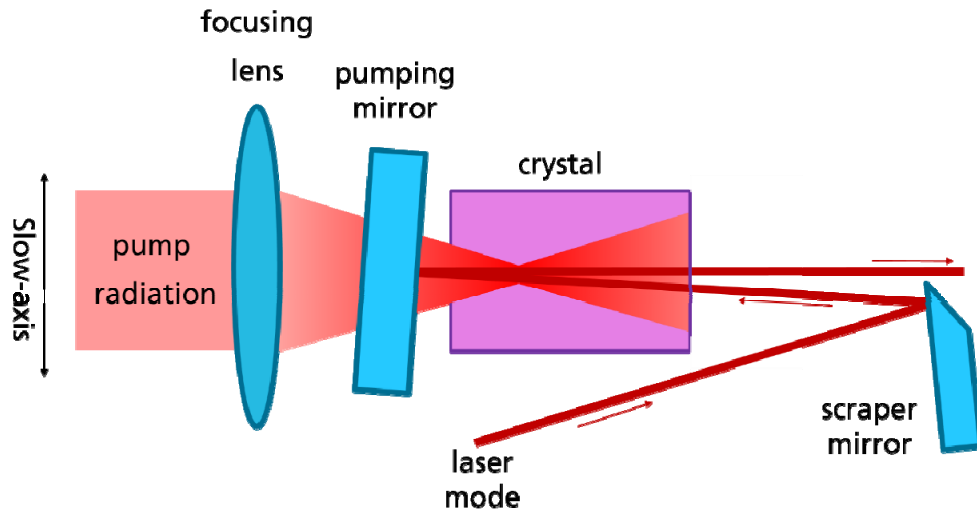


Fig. 2. Scheme of the pump configuration: the pump light is focused through the pumping mirror into the crystal by the focusing lens. Because of the lower beam quality, the divergence in the direction of the slow-axis is much stronger compared to the fast-axis. The laser mode, which is matched in its size to the pump beam size in the fast-axis, passes the laser medium under a small angle in the direction of the slow-axis and is redirected through the crystal along the optical axis by the pumping mirror. Due to the small angle between incoming and outgoing beam, the two can be separated after the laser medium with a scraper mirror.

The asymmetric pump spot in the laser crystal and the different beam qualities in the spatial directions result in a thermal lens with significantly different focal lengths in the two lateral directions. In Q-switched operation with a pump peak power of 100 W and a duration of 200  $\mu$ s at a repetition rate of 150 Hz, we deduced focal lengths of approximately 200 mm focal length in fast-axis and 2500 mm in slow-axis by calculating backwards from the measured laser caustic. The resonator is therefore stable only for small changes of the pump power from the designed working point. For the scaling of the pump power within the performance limitation of the diode modules, the curved mirrors and distances have to be adapted.

To reach the necessary pulse energy, two Alexandrite crystals, each pumped by one laser module, are used for the ring laser. The Alexandrite crystals used as laser media have a length of 7 mm with a  $\text{Cr}^{3+}$ -doping concentration of 0.2 at%, absorbing more than 95% of the incident pump light. For optimized laser performance at the required output wavelength, the Alexandrite crystals are operated at elevated temperatures. In our setup, the best laser performance is observed at 115  $^{\circ}\text{C}$  for an output wavelength of 770 nm.

The setup of the resonator is shown in Fig. 3. It comprises two dichroic pumping mirrors with high transmission for the pump wavelength, several highly reflective mirrors for the laser wavelength, a Brewster angle Pockels cell and a thin-film polarizer to allow Q-switching, a half-wave plate, a Faraday rotator for unidirectional operation and a plane output coupler with 3% transmission for the laser wavelength. The total length of the resonator is approximately 1000 mm. The distance between the two laser media is 170 mm, between the laser media and the curved mirrors it is 280 mm, and between both curved mirrors it is 310 mm. One of the plane mirrors is mounted in a mirror mount with piezo-driven adjusters so that the resonator can be adjusted remotely. To compensate for the stronger thermal lens in fast-axis, one of the pump mirrors is a highly reflective convex cylindrical mirror with a radius of curvature of + 200 mm in the direction of the fast-axis. The spherical curved mirrors have radii of curvature of  $-1000$  mm and  $-750$  mm, respectively. The resonator is designed for a laser beam radius of around 200  $\mu$ m in the crystals with slight differences in



the two laser media because of the different radii of curvature of the resonator mirrors. The beam radius on the optical components like the Pockels cell or the Faraday rotator is around  $400\ \mu\text{m}$ . Thereby, a good overlap with the pump beam is guaranteed and laser induced damage is prevented. A photo of the operating ring resonator is shown in Fig. 4.

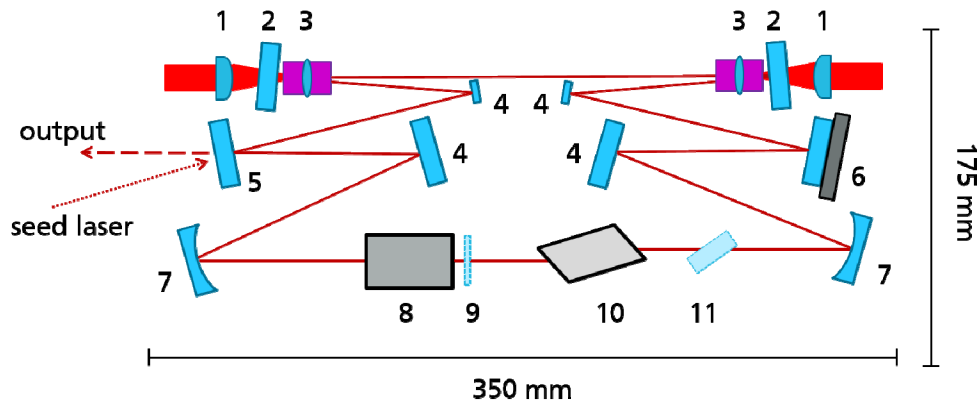


Fig. 3. Schematic setup of the ring cavity with numbered cavity elements: Focusing lens (1), pumping mirror (2), Alexandrite crystal with intrinsic thermal lens (3), flat folding mirrors (4), output coupler (5), mirror on piezo actor for stabilization of the cavity length (6), curved mirror (7), Faraday Rotator (8), half-wave plate (9), Brewster Pockels cell (10), thin-film polarizer (11).

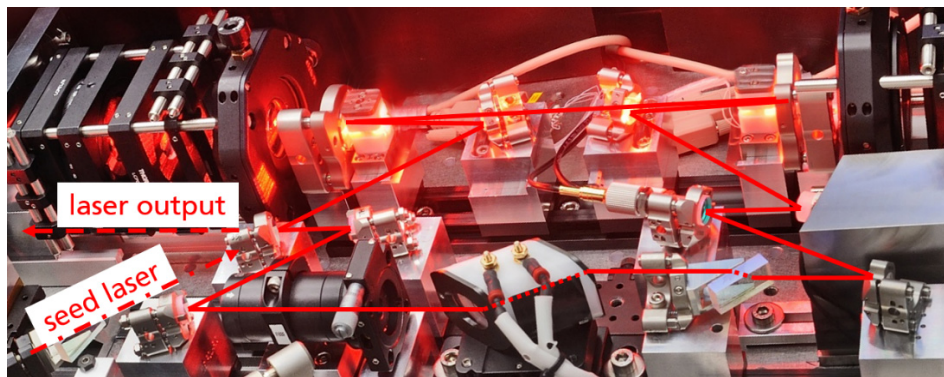


Fig. 4. Photograph of the ring cavity with the beam path sketching in red.

SLM operation of the Alexandrite laser is achieved by a commercial external cavity diode seed laser that operates at the desired wavelength in cw SLM operation. The linewidth of the seed laser is  $< 1\ \text{MHz}$  and the output power is about 20 mW. To achieve SLM operation, the seed laser must be spatially matched with the resonator mode and the cavity length has to be matched to the desired wavelength. In this case, the cavity length is adjusted by one of the plane resonator mirrors, marked with number 6 in Fig. 3, which is mounted on a piezo actuator so that stabilized SLM operation can be achieved using the ramp-and-fire method described in [21].

#### 4. Experimental results

The following experimental results were achieved in SLM operation with a pump pulse duration of  $170\ \mu\text{s}$ , a pump current of 20 A and a repetition rate of 150 Hz. The laser yields,



as shown in Fig. 5 (a), a pulse energy of 1.1 mJ with a standard deviation of 5%, which complies with the requirements of the measurement. The energy of every pulse is measured and taken into account for the calculation.

The laser beam has a Gaussian beam profile, as shown in Fig. 5 (b), and a beam quality of  $M^2_x = 1.16$  and  $M^2_y = 1.15$ . After beam shaping by means of cylindrical lenses, the beam profile of the laser is round and stigmatic. The Faraday rotator inside the resonator ensures reliable unidirectional operation and the polarization of the emitted light is 100% linear. When the electric efficiency of about 33% of the diode modules is taken into account, the electrical-to-optical efficiency of the whole laser system is  $> 1\%$ , a significant improvement compared to the flashlamp-pumped Alexandrite laser used in [4], which has an electrical-to-optical efficiency of 0.03%. The increased efficiency of the laser system means that less heat is generated and that the power consumption of the whole system decreases. Therefore, the increased efficiency of the laser system allows for the design and construction of significantly less complex and smaller lidar systems.

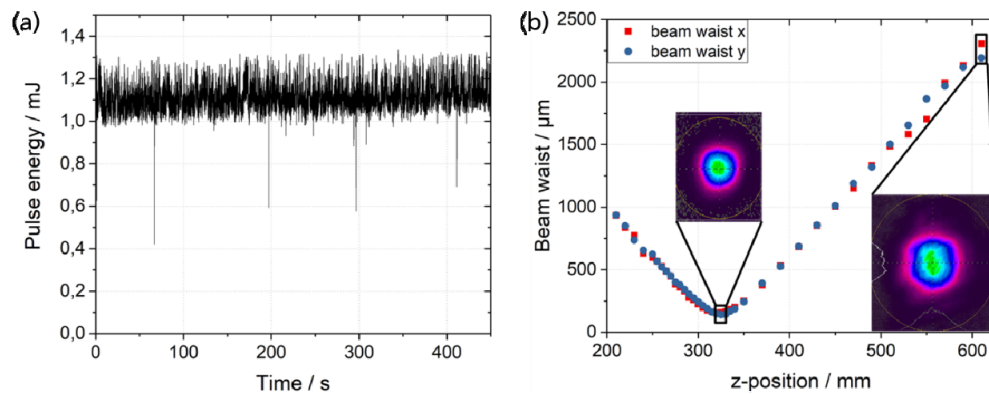


Fig. 5. (a) Pulse energy in SLM operation over time. (b) Caustic of the laser in single longitudinal mode operation after cylindrical beam shaping with beam profiles in focus and far field.

The output wavelength of the unseeded oscillator is 769 nm with a broadband substructure over 1.5 nm. Seeding the cavity and stabilizing the cavity length with the use of the ramp-and-fire method decreases the linewidth significantly, resulting in a linewidth below the spectral resolution of the spectrometer (4 pm or 2 GHz), shown in Fig. 6 (a). Laboratory measurements of the linewidth of the laser after integrating the laser in a novel lidar system indicate a linewidth of approximately 10 MHz. Figure 6 (b) shows the temporal shape of the pulse which has a pulse width of 420 ns with the pulse build-up time being approximately 5 μs.



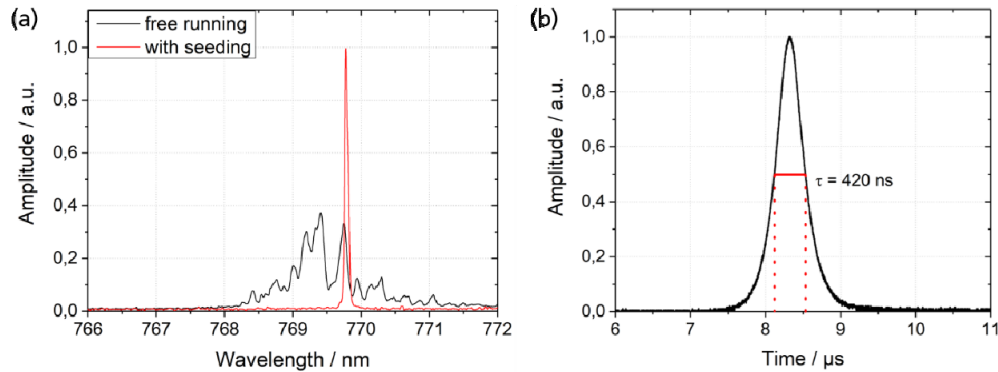


Fig. 6. (a) Optical spectrum of the Q-switched ring laser with and without seeding. (b) Pulse shape in single-longitudinal mode operation.

Additionally, the repetition rate can be scaled up to 320 Hz without any change of the resonator optics. At this repetition rate the pump pulse duration is reduced to 135  $\mu$ s, corresponding to a total pump pulse energy of 26 mJ. This results in a slightly lower pulse energy of 0.65 mJ and longer pulse durations of 800 ns while SLM operation and the spatial beam profile is sustained. With these parameters, 4 MHz linewidth has been achieved.

Figure 7 shows the first atmospheric measurements conducted within a mobile lidar system at the Leibniz IAP in Kühlungsborn, proving the suitability of the laser. Despite the tentative setup of the receiver of the lidar system, the detected light indicates the potassium layer at a height of 80 to 100 km. Detailed information on these measurements and the lidar system will be published soon.

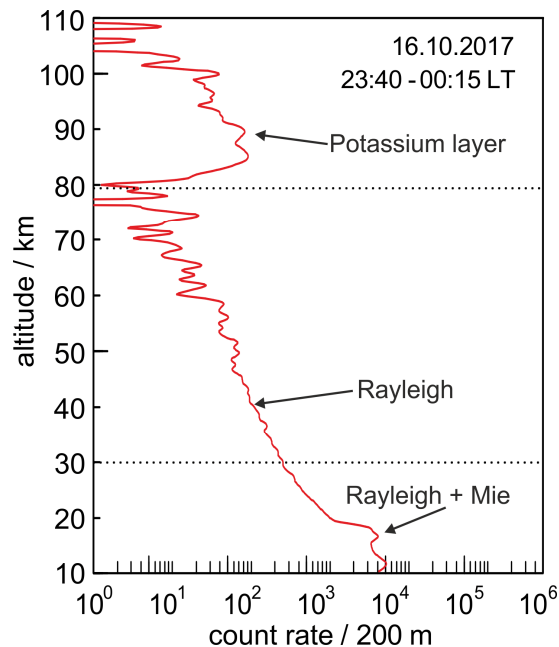


Fig. 7. First atmospheric measurements of the potassium layer with the diode-pumped alexandrite laser.

## 5. Summary and outlook

In this work we presented, to the best of our knowledge, the first demonstration of a diode-pumped Alexandrite ring laser in single longitudinal mode operation. Pulse energies in the



millijoule range at 150 Hz are achieved with a beam quality of  $M^2 < 1.2$  in both spatial directions and a linewidth of  $< 10$  MHz. The laser yields an electric-optical-efficiency of 1% and is, therefore, expected to replace flashlamp-pumped lasers, which are currently used for potassium resonance measurements, but have much lower efficiencies of around 0.03%. First atmospheric measurements could be conducted and prove the high potential of diode-pumped Alexandrite lasers for this application. Our investigation provides initial insight into correctly choosing meaningful design parameters to obtain optimum performance of a diode-pumped Alexandrite laser for resonance lidar systems.

### **Funding**

German Aerospace Center (DLR), Federal Ministry for Economic Affairs and Energy (BMWi) (FKZ 50RP1605).